

Cluster aggregation model for discontinuous percolation transition

Y.S. Cho, B. Kahng and D. Kim

*Department of Physics and Astronomy,
Seoul National University, Seoul 151-747, Korea*

(Dated: March 16, 2019)

Abstract

The evolution of the Erdős-Rényi (ER) network by adding edges can be viewed as a cluster aggregation process. Such ER processes can be described by a rate equation for the evolution of the cluster-size distribution with the connection kernel $K_{ij} \sim ij$, where ij is the product of the sizes of two merging clusters. Here, we study more general cases in which K_{ij} is sub-linear as $K_{ij} \sim (ij)^\omega$ with $0 \leq \omega < 1/2$; we find that the percolation transition (PT) is discontinuous. Moreover, PT is also discontinuous when the ER dynamics evolves from proper initial conditions. The rate equation approach for such discontinuous PTs enables us to uncover the mechanism underlying the explosive PT under the Achlioptas process.

PACS numbers: 64.60.ah, 02.50.Ey, 89.75.Hc

Irreversible cluster aggregations are widespread phenomena occurring in a diverse range of fields, including dust and colloid formation, aerosol growth, droplet nucleation and growth, gelation transition, etc [1]. The Smoluchowski coagulation equation (SCE) [2, 3, 4] can successfully describe such cluster aggregation processes. In linear polymerization, molecules with two reactive ends can react to form long chains. In this case, the reaction kernel is given as $K_{ij} = 1$, where i and j are the masses of the two reactants. For the aggregation of branched polymers, the reaction kernel is has the form $K_{ij} = (ai + b)(aj + b)$, where a and b are constants. When clusters have a compact shape, the reaction kernel has the form $K_{ij} \sim (ij)^{1-1/d}$, where d is the spatial dimension. Intensive studies have been carried out using the SCE with such different kernel types [1, 5, 6, 7, 8], and it is known that sol-gel transitions can occur at either finite or infinite transition points. They are continuous transitions.

During the past decade, the evolution of complex networks has been of much interest to the science communities in multidisciplinary fields. To study percolation transition (PT) during network evolution, the branching process approach [9, 10] and the Potts model formalism [11] have been used. Such complex network evolution can also be viewed as a cluster aggregation phenomenon, and that it can be studied by the rate-equation approach. For example, in the evolution of the classical random network, called the Erdős-Rényi (ER) model, an edge is added in each time step, thereby either connecting two separate clusters (inter-cluster edge) or increasing the edge number in one cluster without changing cluster numbers (intra-cluster edge). Fig. 1(a) shows that the frequency of inter-cluster connections is dominant until the percolation threshold. Thus, the cluster aggregation picture of the ER network evolution comes in naturally. In this Letter, we extend the cluster aggregation dynamics in networks to more general cases. Specifically, the model is as follows: In a system composed of N vertices, we perform the following tasks at each time step.

- Two clusters of sizes i and j are chosen with probabilities q_i and q_j , respectively. The two clusters can be the same. Probability q_i is given as $k_i / \sum_s k_s n_s$, where k_i and n_i are the weight and density of an i -size cluster, respectively.
- Two vertices are selected randomly from the selected clusters. If they are not yet connected, then they are connected. Alternatively, we can choose another pair of vertices from the clusters. Self-loop cases are excluded.

We repeat these simple steps until a given time $t \equiv L/N$, where L , the number of edges added to the system, is tuned. This model is called the cluster aggregation network (CAN) model hereafter. In this model, the two selected clusters can be the same, and thus, the evolution can proceed even after one giant cluster remains. The ER network corresponds to the case $k_i = i$. Here, we show that when the weight is sub-linear, as $k_i = i^\omega$ with $0 \leq \omega < 1/2$, a discontinuous PT can occur at a finite transition point. Moreover, under certain initial conditions, the ER dynamics also exhibits a discontinuous PT. This observation is remarkable, because a discontinuous PT has rarely been discovered in irreversible kinetic systems, except for recent observations in the ER [13] and other networks [14, 15, 16] under the so-called Achlioptas process (AP) [13]. The results obtained from the CAN model help us to understand the mechanism that underlies the explosive PT under the AP.

The cluster aggregation processes in the CAN model are described via a rate equation for the cluster density, which takes the following form in the thermodynamic limit:

$$\frac{dn_s(t)}{dt} = \sum_{i+j=s} \frac{k_i n_i}{c(t)} \frac{k_j n_j}{c(t)} - 2 \frac{k_s n_s}{c(t)}, \quad (1)$$

where $c(t) = \sum_s k_s n_s(t)$. The connection kernel $K_{ij} \equiv k_i k_j / c^2$. The first term on the right hand side represents the aggregation of two clusters of sizes i and j with $i + j = s$ and the second term represents a cluster of size s merging with another cluster of any size. The rate equation differs from SCE in two aspects. First, the connection kernel is time-dependent through $c(t)$ when $\omega \neq 1$. Second, the second term on the right hand side of Eq. (1) includes the process of merging with an infinite-size cluster. Hence, Eq. (1) with $\omega = 1$ and $c = 1$ describes the ER process, while SCE with $\omega = 1$ does not. Owing to the presence of $c(t)$, a PT occurs at a finite transition point even when a PT does not occur in the SCE, for example, when $\omega = 0$. Here, we study the cases $k_i = 1$ ($\omega = 0$), $k_i = i^\omega$ with $0 < \omega < 1$, and $k_i = i$ ($\omega = 1$), separately.

The case $\omega = 0$: In this case, $c(t) = \sum_s n_s$ becomes the total density of the clusters, which decreases linearly with time. The generating function of $n_s(t)$ is defined as $f(z, t) = \sum_s n_s(t) z^s$, where z is the fugacity in the range $0 < z < 1$. Then, one can obtain the differential equation for $f(z, t)$ from Eq. (1) and solve in a closed form as $f(z, t) = (1 - t)^2 z / (1 - zt)$ for $t < 1$ and 0 for $t > 1$. Expanding $f(z, t)$ as a series in z , we obtain $n_s(t) = (1 - t)^2 t^{s-1}$ in the thermodynamic limit. This formula shows that the cluster size distribution decays exponentially as s becomes large. Particularly, when

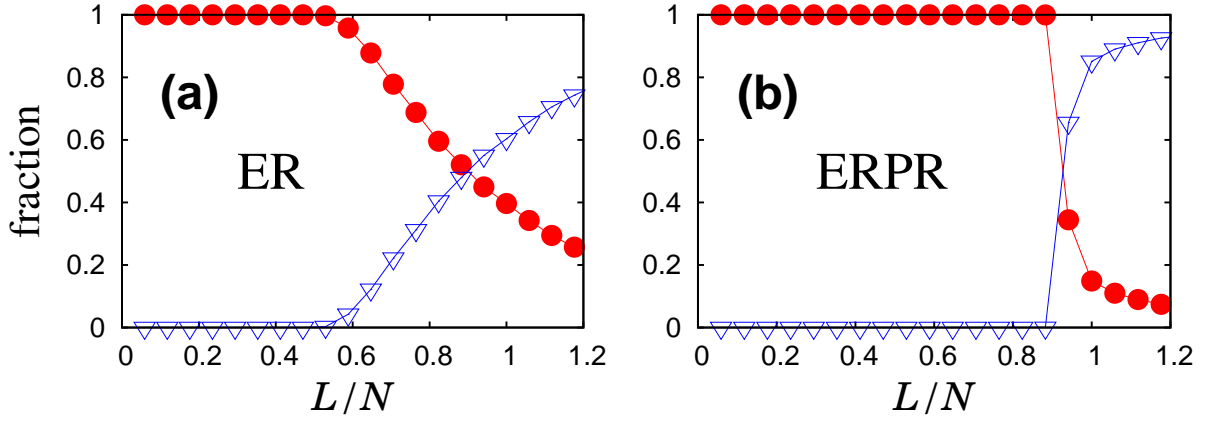


FIG. 1: (Color online) The fraction of each type of attached edges, inter-cluster (\bullet) or intra-cluster (∇) edges for (a) the ER and (b) the ERPR network. While the fraction of inter-cluster connections after t_c decays slowly in (a), it does so rapidly in (b).

$\delta \equiv 1 - t$ is small, $n_s(\delta) \approx \delta^2 e^{-s/s^*}$ with $s^* \approx 1/\delta$. The characteristic size s^* diverges as $\delta \rightarrow 0$. As shown in the inset of Fig. 2(a), $n_s(t)$ is almost flat, indicating that large-size clusters are relatively abundant. The merging of these clusters causes a sudden jump in the giant cluster size, leading to a first-order transition.

We find the giant cluster size $G(t)$ by using the relation, $G(t) = 1 - f'(1, t) \equiv 1 - \sum'_s s n_s(t)$, where the summation excludes an infinite-size cluster. We find that $G(t) = 0$ for $0 < t < 1$ and 1 for $t > 1$ (Fig. 3(a)). Thus, the PT is first-order at $t_c = 1$. This result differs from what we obtain from the SCE, in which transition point $t_c = \infty$.

The case $0 < \omega < 1$: For this case, while an exact solution is not possible, $n_s(t_c)$ is obtained under some assumption. To proceed, we define the generating function $h(z, t) \equiv \sum_s s^\omega n_s(t) z^s / c(t)$, and presume that $n_s(t_c) \sim s^{-\tau}$. Next, we use the assumption made in Ref. [5, 7] for the SCE that $n_s(t) = n_s(t_c) / (1 + b(t - t_c))$ near $t = t_c^+$, where b is an s -independent constant. Then, comparing the most singular terms in the series of the generating functions $f(z, t_c)$ and $h^2(z, t_c)$ in $1 - z$, we find that $\tau = 1 + 2\omega$ for $0 < \omega < 1/2$ and $\tau = 3/2 + \omega$ for $1/2 < \omega < 1$. This result is confirmed numerically. When $t < t_c$, $n_s(t)$ follows a power-law function with an exponential cutoff for $1/2 < \omega < 1$, but it exhibits a hump in a large-size region for $0 < \omega < 1/2$ (Fig. 2(b)).

We examine $G(t)$ as a function of time for various ω cases. $G(t)$ exhibits a transition at finite t_c , which is continuous for $1/2 < \omega \leq 1$, discontinuous for $0 \leq \omega < 1/2$ (Fig. 3),

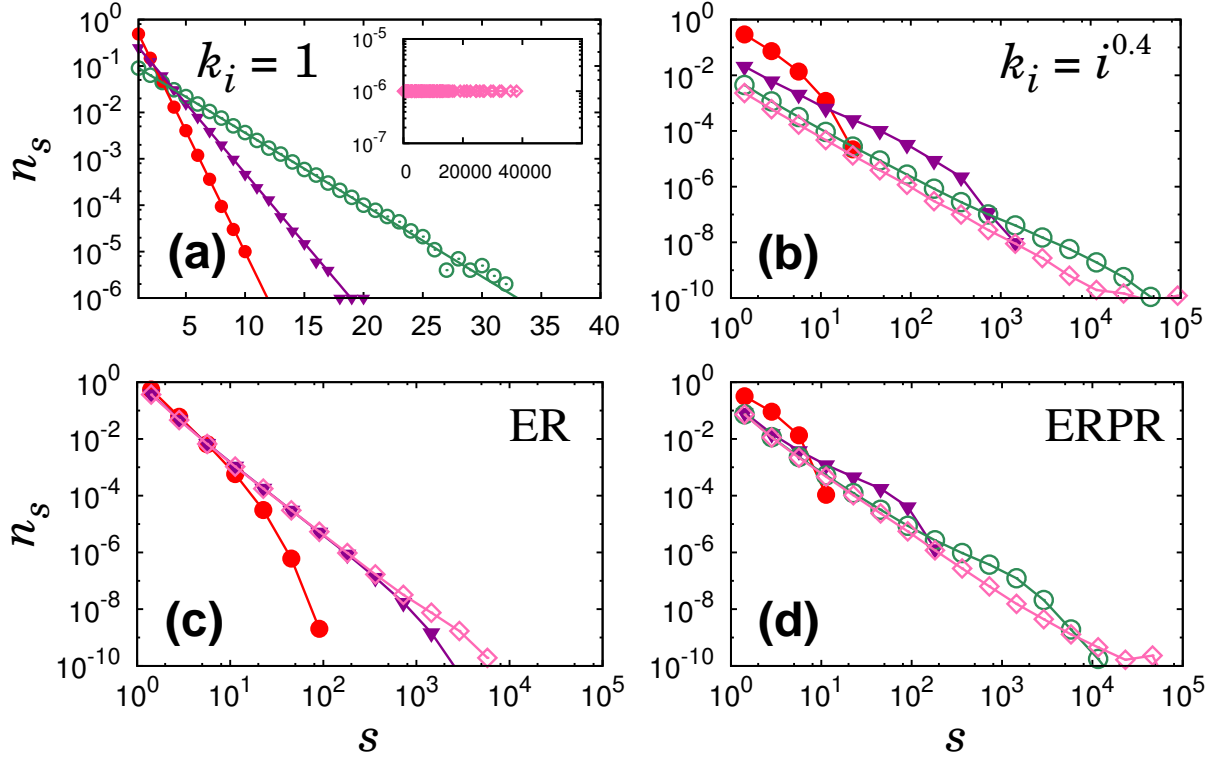


FIG. 2: (Color online) The cluster-size distributions of the CAN models with (a) $k_i = 1$, (b) $k_i = i^{0.4}$, (c) $k_i = i$ (ER model), and (d) the ERPR network. (a) is drawn in semi-logarithmic scale, while the others are in double-logarithmic scales. The data points in (a) are at $t/t_c = 0.3(\bullet)$, $0.5(\nabla)$ and $0.7(\circ)$, and in (b), (c), and (d), they are obtained at $t/t_c = 0.50(\bullet)$, $0.95(\nabla)$, $0.998(\circ)$, and $1.003(\diamond)$. Data points in the inset of (a) are at $\delta = 1 - t = 10^{-4}$. In (b) and (d), there exist humps for data points (\circ) . The system size is taken as 10^6 for (a) and $N = 10^5$ for (b), (c), and (d).

and marginal for $\omega = 1/2$. The first-order transition is tested in Fig. 4 using the scaling approach introduced in Ref. [13]. We define $\Delta \equiv t_1 - t_0$, where t_0 and t_1 are chosen in the function $G(t)$ as the times at which the value of G reaches $1/\sqrt{N}$ and 0.8 for the first time, respectively. We find numerically that when $\omega = 0.4$, there exists a scaled quantity $\Delta N^{0.21}$, which is independent of N . Since $\Delta \rightarrow 0$ as $N \rightarrow \infty$, the transition is discontinuous. When $\omega = 0.8$, however, Δ converges to a finite value as $N \rightarrow \infty$. Thus, the transition is continuous.

The case $\omega = 1$: This case is exactly solvable as the case of the SCE [6]. We consider an

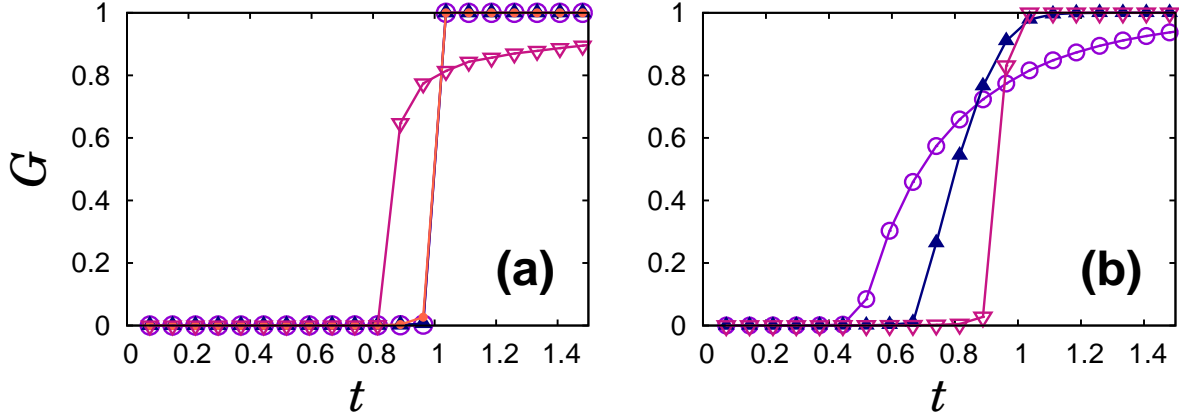


FIG. 3: (Color online) The density of the giant cluster size G versus time t showing (a) discontinuous transitions in $k_i = 1$ (\circ), $k_i = i^{0.2}$ (\triangle), $k_i = i^{0.4}$ (\bullet), and the ERPR model (∇) and (b) continuous transitions in the CAN model $k_i = i^{0.6}$ (∇), $k_i = i^{0.8}$ (\triangle), and the ER network (\circ).

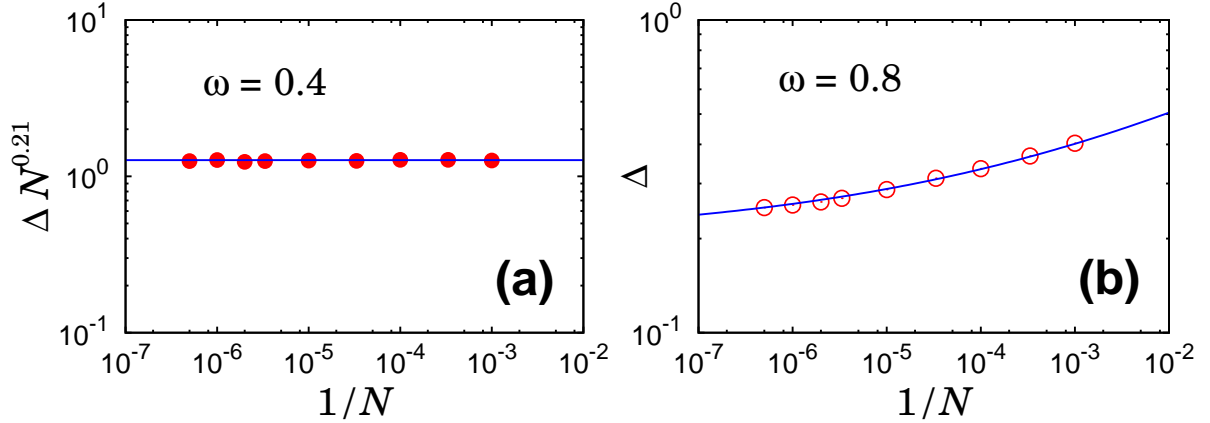


FIG. 4: (Color online) Test of the discontinuous or continuous PT for the CAN models with (a) $\omega = 0.4$ and (b) $\omega = 0.8$. In (a), the flat behavior implies that $\Delta \equiv t_1 - t_0$ decreases with the rate $\sim N^{-0.21}$, while $G(t_1) - G(t_0)$ remains constant in $\mathcal{O}(1)$. Thus, the transition is of the first order. In (b), the data tend to converge to a constant with increasing N , which implies that Δ remains constant, and that the transition is continuous.

arbitrary initial condition of $n_s(0)$. In this case, $c(t) = \sum_s s n_s(t)$ is conserved, but the first moment $m_1(t) = \sum'_s s n_s(t)$, with the sum excluding the largest cluster, is not. When we define the generating function $g(\mu, t) \equiv 1 - \sum_s s n_s(t) \exp(-\mu s)$, it is given by the solution of $g(\mu, t) = H(\mu + 2tg(\mu, t))$ where $H(x) \equiv g(x, 0)$ is fixed by the initial conditions of $n_s(0)$.

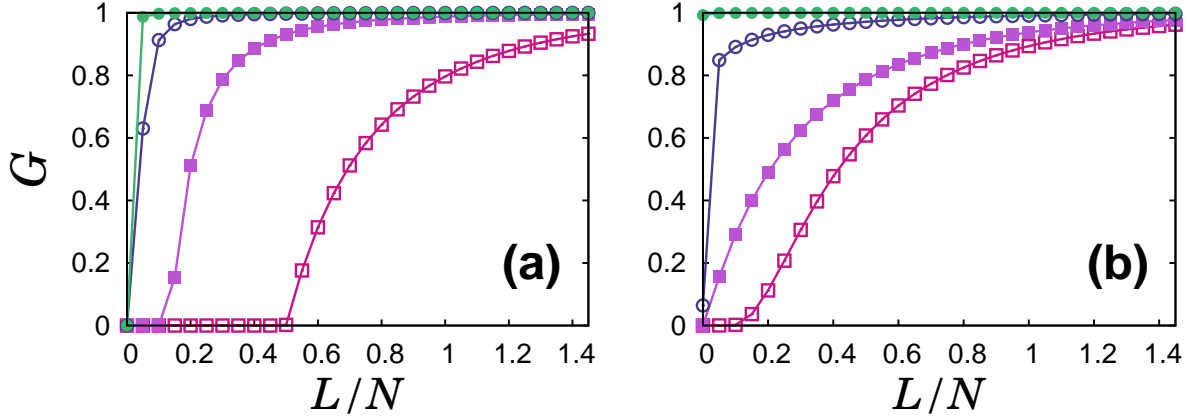


FIG. 5: (Color online) Plot of the density of the giant cluster size G versus time for the ER network with different initial conditions. In (a), the cluster-size distribution $n_s(0)$ is flat with different cutoff values $s_m = N^\alpha$, with $\alpha = 0, 0.1, 0.2$, and 0.3 from right to left. In (b), $n_s(0)$ decays according to a power law with exponent $\tau = 3, 2.5, 2$, and 1.5 from right to left.

From this, one finds that the second moment $m_2(t) \equiv \sum'_s s^2 n_s(t)$ behaves as

$$m_2(t) = \frac{m_2(0)}{1 - 2m_2(0)t}. \quad (2)$$

for $t < t_c = 1/(2m_2(0))$. $G(t)$ is the non-zero solution of $G = H(2tG)$ and is obtained near t_c as

$$G(t) = \frac{2m_2^2(0)}{m_3(0)} (2m_2(0)t - 1), \quad (3)$$

where $m_3(0) = \sum'_s s^3 n_s(0)$ is the initial third moment. These solutions for arbitrary initial conditions are later used to study the first-order transition in the ER network under the AP. For the CAN model, the initial condition is $n_s(0) = \delta_{s,1}$. Then, $m_2(0) = m_3(0) = 1$, and consequently, $t_c = 1/2$, which is the well-known ER value. The giant cluster size exhibits a continuous transition at t_c with $n_s(t_c) \sim s^{-5/2}$.

For the following discussion, we consider the two cases in which $m_2(0)$ and $m_3(0)$ depend on N . First, we assume that $n_s(0)$ follows a flat distribution, $n_s(0) = s_0$, in the range $0 < s < s_m$, where s_m , the size of the largest cluster, depends on N as $s_m = N^\alpha$. Then, $s_0 = 2N^{-2\alpha}$, $m_2(0) \propto N^\alpha$, and $m_3(0) \propto N^{2\alpha}$. Then, a PT takes place at $t_c(N) = 1/2m_2(0) \propto N^{-\alpha}$, and $G(t) \sim r(2m_2(0)t - 1)$ for $t > t_c(N)$ from Eq. (3), where r turns out to be in $\mathcal{O}(1)$. Thus, if time t is scaled as $t' = tm_2(0)$, then $G(t')$ is the solution of $G = \tilde{H}(2t'G)$, where $\tilde{H}(x)$ is a regular function qualitatively similar to $H(x) = 1 - e^{-x}$ for the standard ER problem. Hence,

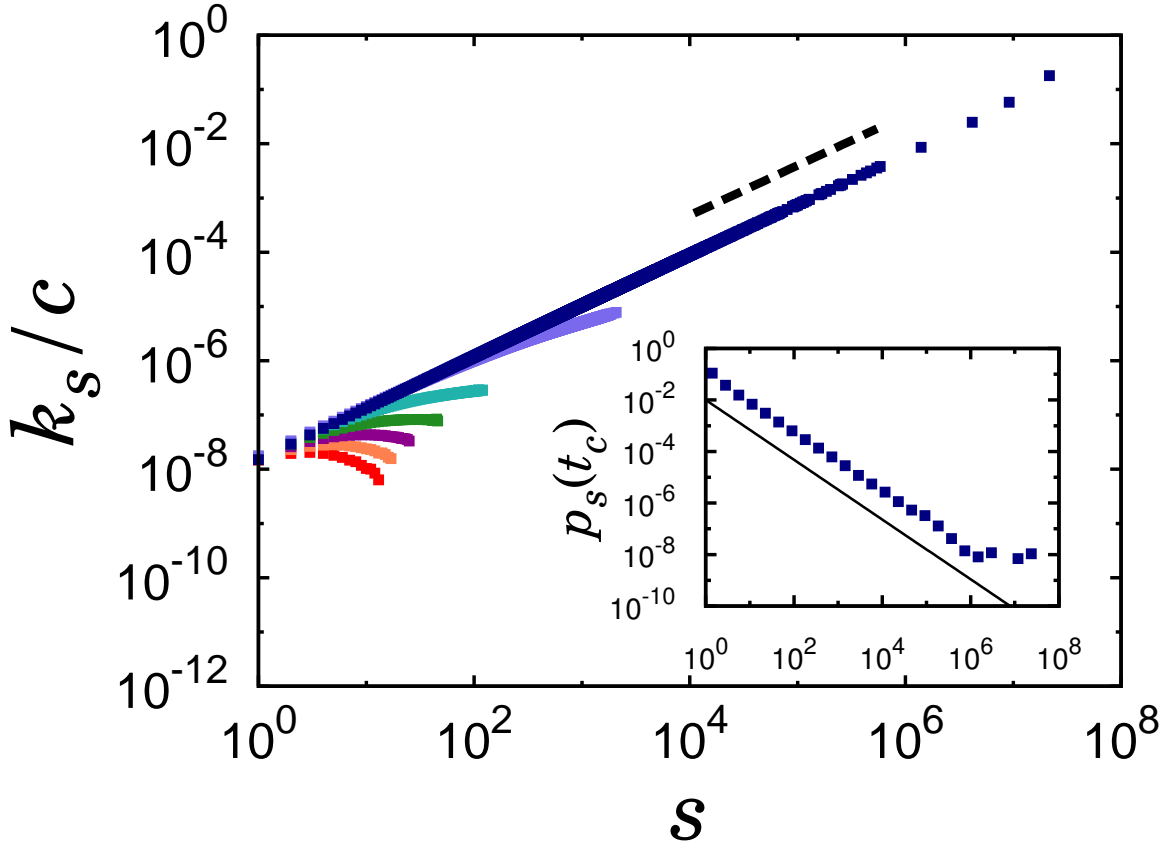


FIG. 6: (Color online) Plot of $k_s/c(t)$ versus s at various times for an ERPR network with system size $N = 10^8$. The dashed line is a guideline with slope 0.92. Data are for $t = 0.4, 0.5, 0.6, 0.7, 0.8, 0.88(\approx 0.99t_c(N))$, and $0.889 (= t_c(N))$ from the bottom. Inset: Plot of $p_s(t_c(N))$ versus s at $t_c(N)$. The solid line is a guideline with slope -1.2 .

$G(t')$ has a mean field behavior similar to the original ER case. This scaling behavior implies that while $\delta G(t) \equiv G(t_1) - G(t_0)$ increases by $\mathcal{O}(1)$, $\Delta \equiv t_1 - t_0$ does so by $\sim \mathcal{O}(N^{-\alpha})$. Thus, we have a first-order transition as $N \rightarrow \infty$ (Fig. 5(a)). Second, when $n_s(0) \sim s^{-\tau}$ with an N -dependent cutoff, we can show analytically that a similar first-order transition occurs at $t_c(N)$ when $\tau \leq 2$. When $\tau > 2$, however, a continuous transition occurs either at a finite transition point t_c ($\tau > 3$) or at a trivial point $t_c = 0$ ($2 < \tau < 3$) (Fig. 5(b)).

The AP case: The network evolution under the AP proceeds as follows: At each time step, we select two candidates of edges randomly, and then select the one that has the lower value for the product of the sizes of the two clusters that the edge is joining, which is called the product rule (PR). The selected edge is added to the system. The ER network under

the AP with the PR is called the ERPR network. The evolution of ERPR networks can also be regarded as cluster aggregation processes (Fig. 1(b)), but with a complicated and possibly time-dependent kernel K_{ij} (Fig. 6).

The cluster-size distribution $n_s(t)$ is measured in Fig. 2(d). As t passes and reaches close to t_c^- , it develops a hump in a large-size region, indicating an abundance of large-size clusters. As t reaches the transition point $t_c(N)$ where the slope of G versus t is maximum at finite N , such clusters finally condense into one giant cluster, and the density of the remaining finite-size clusters exhibits a power-law behavior $n_s \sim s^{-\tau}$ with $\tau \approx 2.1(1)$, which differs from the exponent value $\tau_{\text{ER}} = 2.5$ for the ER case. Taking account of the presence of a hump in a tailed region, the exponent value $\tau \approx 2.1(1)$ may be reduced further, which is meaningful for further discussion.

To observe the dynamics of ERPR networks at the microscopic level, we measure the probability $p_s(t) = q_s n_s(t) = k_s n_s(t)/c(t)$ that an added edge is connected to a vertex within an s -size cluster at time t . Using the measured $p_s(t)$ and $n_s(t)$, we calculate $q_s = k_s/c(t)$, which behaves as $\sim s^\omega$ asymptotically as $t \rightarrow t_c^-$. The exponent ω depends on time (Fig. 6), for example, ω is increased as much as $\omega \approx 0.88(1)$ at $t/t_c(N) = 1 - 10^{-4}$ and $\omega \approx 0.92(1)$ at $t = t_c(N)$ for $N = 10^8$. The closeness of the ω value to $\omega = 1$ indicates that the short time dynamics near t_c proceeds similarly to that in the ER network. Fortunately, this property enables us to understand the first-order transition in the ERPR network within the framework of the ER model, which is discussed later. On the other hand, p_s at t_c exhibits a power-law behavior in a wide range of s as $\sim s^{-1.2}$ (Inset of Fig. 6), which decays more slowly than the one, $\sim s^{-1.5}$, in the ER case. This fact indicates that large-size clusters are more abundant in the ERPR case than in the ER case. In the CAN model with $0 < \omega < 1$, $p_s(t_c)$ behaves as $\sim s^{-(1+\omega)}$ when $0 < \omega < 1/2$ and as $\sim s^{-3/2}$ when $1/2 < \omega \leq 1$. Thus, the observed result, $p_s(t_c) \sim s^{-1.2}$, in the ERPR case belongs to the case $0 < \omega < 1/2$. These all show first-order PTs.

Let us see what happens to the dynamics of the ERPR network as $t \rightarrow t_c^-$. We choose a certain time $t^*(N)$, for example t_0 as previously defined. At that time, the exponent ω does not grow as much as $\omega_{\text{ERPR}} \approx 0.9$ obtained at $t_c(N)$. Now we assume that the network evolves by the ER process ($\omega = 1$ of the CAN) from this time on for a short period. The size of G in this process would be larger than that of the original ERPR process but during the short interval evolution, the difference would not be large. We take $t^*(N)$ as the origin of

time, and $n_s(t^*)$ as the initial condition, where $n_s(t^*)$ is obtained from the ERPR dynamics. Then, we apply this situation to the aforementioned argument related to formulae (3) and (4). We obtain $m_2(t^*(N)) \sim N^{0.43(1)}$ and $m_3(t^*(N)) \sim N^{0.87(1)}$. Then, the condition that m_2^2/m_3 is finite and m_2 increases with N is fulfilled. Moreover, $n_s(t^*(N)) \sim s^{-\tau}$ with τ being around or smaller than 2 (reduced by the presence of a hump), satisfying the criterion $\tau < 2$. Thus, the transition is first-order. We find that as t^* approaches t_c further, the first-order transition criterion continues to hold. This shows why a first-order transition takes place in the ERPR network. Just before the transition, the ERPR product rule prepares a large number of finite but large clusters, as seen in the hump of Fig. 2(d) with diverging $m_2(t^*)$ but with finite $m_2^2(t^*)/m_3(t^*)$. Then, a small further addition of links, ER-like or not, produces the explosion in the small time interval of $m_2^{-1}(t^*)$.

In summary, we have introduced a cluster aggregation network (CAN) model, in which discontinuous percolation transitions occur when the connection kernel is sub-linear as $K_{ij} \sim (ij)^\omega$ with $0 \leq \omega < 1/2$. Even for the ER network, a discontinuous PT can be obtained by using initial conditions where $m_2(0)$ diverges and $m_2^2(0)/m_3(0)$ remains finite. Since the CAN model evolves by single-edge dynamics, as compared to the ERPR, which involves a pair of edges at each time step, it was helpful to study the ERPR model within the scheme of the CAN model. We measured the connection kernel of the ERPR network and found that the mapping from ERPR to ER is possible as $t \rightarrow t_c^-$. Examining the cluster-size distribution of the ERPR, we found that the underlying mechanism of the explosive PT in the ERPR model was within the category of the first-order transition of the ER model under the *ad hoc* initial condition. We expect that the CAN model can be used to study scaling properties [17] in a discontinuous PT; this is a matter for further studies.

This work was supported by a KOSEF grant Acceleration Research (CNRC) (Grant No.R17-2007-073-01001-0) and by the NAP of KRCF.

-
- [1] *Kinetics of aggregation and gelation*, edited by F. Family and D.P. Landau, (North-Holland, Amsterdam, 1984).
 - [2] M.V. Smoluchowski, *Physik. Zeits.* **17**, 557 (1916).
 - [3] P.J. Flory, *J. Am. Chem. Soc.* **13**, 3083 (1941).

- [4] W.H. Stockmayer, J. Chem. Phys. **11**, 45 (1943).
- [5] R.M. Ziff, E.M. Hendriks, and M.H. Ernst, Phys. Rev. Lett. **49**, 593 (1982).
- [6] R.M. Ziff, E.M. Hendriks, and M.H. Ernst, J. Phys. A: Math. Gen., **16**, 2293 (1983).
- [7] F. Leyvraz and H.R. Tschudi, J. Phys. A **14**, 3389 (1981).
- [8] F. Leyvraz, Phys. Rep. **383**, 95 (2003).
- [9] D.S. Callaway, M.E.J. Newman, S.H. Strogatz, and D.J. Watts, Phys. Rev. Lett. **85**, 5468 (2000).
- [10] R. Cohen, D. ben-Avraham, and S. Havlin, Phys. Rev. E **66**, 036113 (2002).
- [11] D.S. Lee, K.-I. Goh, B. Kahng, and D. Kim, Nucl. Phys. **B696**, 351 (2004).
- [12] P. Erdős, A. Rényi, Publ. Math. Hugar. Acad. Sci. **5**, 17 (1960).
- [13] D. Achlioptas, R. M. D'Souza, and J. Spencer, Science **323**, 1453 (2009).
- [14] R. M. Ziff, Phys. Rev. Lett. **103**, 045701 (2009).
- [15] Y.S. Cho, J.S. Kim, J. Park, B. Kahng, and D. Kim, Phys. Rev. Lett. **103**, 135702 (2009).
- [16] F. Radicchi and S. Fortunato, Phys. Rev. Lett. **103**, 168701 (2009).
- [17] E.J. Friedman and A.S. Landsberg, arXiv:0910.3979.